ORIGINAL PAPER

Impedance study of thiolated polyaniline

**Maija Blomquist · Johan Bobacka · Ari Ivaska ·
Kalle Levon**

Abstract Covalent attachment of thiolated probes to conducting polymers such as polyaniline (PANI) is a promising approach towards the development of electrochemical sensors and biosensors. However, thiolation alters the conjugated polymer backbone and influences the electrochemical behavior of the conducting polymer. PANI studied in this work was electropolymerized on glassy carbon (GC) electrodes from a solution of 0.1 M aniline in 0.5 or 1.0 M H_2SO_4. The GC/PANI electrodes were then functionalized by covalent attachment of 2-mercaptoethanol to the PANI backbone. The progress of thiolation was studied by cyclic voltammetry and electrochemical impedance spectroscopy (EIS). Thiolation of PANI was found to cause an initial decrease in electroactivity at 0–0.25 V and an increase in electroactivity at 0.25–0.6 V. However, prolonged thiolation caused a loss of electroactivity of PANI, which could be seen from EIS measurements as a dramatic decrease in the bulk redox capacitance of PANI.

Keywords Polyaniline · Electrochemical impedance spectroscopy · Alkanethiol · Electropolymerization · Cyclic voltammetry

M. Blomquist · J. Bobacka (✉) · A. Ivaska · K. Levon
Laboratory of Analytical Chemistry, Process Chemistry Centre,
Åbo Akademi University,
Biskopsgatan 8,
20500 Turku/Åbo, Finland
e-mail: johan.bobacka@abo.fi

M. Blomquist
Nanoscience Center, The Finnish National Graduate
School in Nanoscience (NGS-NANO), University of Jyväskylä,
P.O. Box 35, 40014 Jyväskylä, Finland

K. Levon
Chemical and Biological Sciences,
Polytechnic Institute of New York University,
Six Metro Tech Center,
Brooklyn, NY, USA

Introduction

Electrochemical impedance spectroscopy (EIS) is a powerful tool to study electrochemical processes [1]. Conducting polymers are often studied by using EIS, providing information about charge transfer resistance, double layer capacitance and bulk redox capacitance of conducting polymer films [2]. PANI is one of the conducting polymers that awake a lot of interest, e.g., due to its easy synthesis in acidic solutions and high stability. The electrochemistry of PANI is very complex though. It has three different redox states depending on the potential. Leucoemeraldine is the most reduced state, emeraldine state is the oxidized form, and pernigraniline is the overoxidized state. These three states still have their salt and base forms depending on the protonation degree. The only conducting form is emeraldine salt. Polyaniline is sensitive to pH. The sensitivity to pH is less in PANI derivatives, such as *N*- and ring-substituted anilines [3], which also tend to have quite different characteristics compared with PANI [4–7]. PANI has a backbone with an amine group and a benzene ring and both can be functionalized [4, 8]. By substitution, other properties, like the solubility and conductivity of PANI, can also be tailored [4].

Thiolated oligonucleotides can be attached covalently to various surfaces through nucleophilic reaction [9, 10]. This procedure is mostly followed by adding alkyl thiols as spacers that fill the free sites left on the substrate [11]. On gold surfaces, this prevents undesired molecules to bind to the surface and also helps ssDNAs to stay more upright from the surface so that they more easily can react to target DNAs. Conducting polymers offer unique surfaces for attachment and the conducting polymers can work as transducers in various types of chemical sensors [12]. Thiolation has even been used for immobilization of ssDNA on conducting polymer substrates [9, 13].

When alkyl thiols are covalently bound to the benzene ring of polyaniline and form functionalized PANI, this will

affect the electrochemical properties of PANI. The overall effect of thiolation leads to a reduced PANI backbone [13–18]. Aromatic rings will become three-substituted and, depending on the nature of the substituent, steric hindrance will be increased [19]. Furthermore, the redox states and conductivity of PANI depend on the applied dc potentials as well on the pH of the electrolyte [20]. The mechanism of thiolation of PANI was studied recently by FTIR and Raman spectroscopy (Blomquist et al., manuscript submitted for publication). The covalent binding of thiol to PANI is illustrated in Scheme 1. Preliminary studies by cyclic voltammetry (CV) and EIS also revealed interesting changes in the electrochemistry of PANI upon thiolation (Blomquist et al., manuscript submitted for publication).

The objective of the present work is to understand in more detail the impact that covalently bound thiolated probes have on the electrochemical properties of PANI deposited on glassy carbon (GC/PANI). This study is therefore focused on more extensive thiolation which is obtained by potential cycling of GC/PANI electrodes for up to 2,800 cycles in H_2SO_4 containing 0.1 M MCE. In this study, the impedance spectra of the intact (non-thiolated) GC/PANI electrode will be compared with the impedance spectra of GC/PANI that is thiolated with increasing number of cycles in an acidic 2-mercaptoethanol (MCE) solution. The impedance spectra are recorded as a function of the applied dc potentials both in 0.5 and 1.0 M H_2SO_4. This study is relevant concerning further development of such electrochemical sensors and biosensors where receptors are covalently bound to conducting polymers via thiolation.

Experimental

Chemicals

Aniline was obtained from Sigma-Aldrich and distilled before use. H_2SO_4 was obtained from J. T. Baker and diluted with deionized water to desired concentration. 2-Mercaptoethanol was purchased from Aldrich and used as received. Deionized water was used throughout this work. All electrochemical experiments were done at room temperature (23 ± 1 °C).
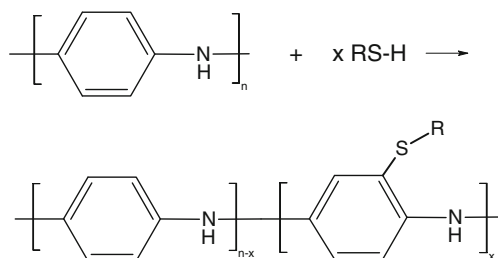
Scheme 1 Thiolation of PANI. The PANI should be in the emeraldine salt/base or pernigraniline base/salt form for the reaction to take place (Blomquist et al., manuscript submitted for publication)

Electropolymerization of aniline

Electropolymerization of aniline was done on glassy carbon disk working electrodes ($A=0.077$ cm^2) in a three-electrode cell. A GC rod served as the counter electrode (CE) and an Ag|AgCl|3 M KCl (Metrohm) as the reference electrode. The electrodes were placed at fixed positions of about 0.5-cm distance from each other and the volume of the electrolyte was 10 ml (total cell volume=30 ml). Prior to electropolymerization, the electrodes were polished with 15, 9, 3, and 1 μm diamond paste (in this order) and with 0.3 μm Al_2O_3 powder, rinsed with deionized water, and dried. Electropolymerization and subsequent cyclic voltammetry were done with an IVIUMSTAT potentiostat (Ivium Technologies, The Netherlands).

Electropolymerization of 0.1 M aniline was done in 0.5 or 1.0 M H_2SO_4 by cycling the potential between −0.15 and 0.75 V for 25 or 50 cycles at a scan rate of 50 mV/s. PANI electropolymerized with 25 and 50 cycles will be referred to as "25-cycle-PANI film" and "50-cycle-PANI film", respectively. Polymerization was initiated by holding the potential at 0.85 V for 10 s before starting the cycling. The second oxidation/reduction couple of polyaniline that can partly destroy the electroactivity of the film can be avoided by this polymerization method [21, 22].

After polymerization, the GC/PANI electrodes were characterized by CV (10 cycles, scan rate=50 mV/s) in a monomer-free solution of the same acid strength as that used in polymerization. Prior to all the measurements, the solutions were purged with nitrogen, and during the measurements nitrogen was passed over the solutions. All the electropolymerizations and CVs were done in a Faraday cage.

Thiolation of polyaniline films

Thiolation of electropolymerized PANI films was done by cycling the GC/PANI electrodes between −0.15 and 0.75 V in a solution of 0.5 M or 1.0 M $H_2SO_4+0.1$ M MCE. The scan rate was 50 mV/s and the number of scans varied between 10 and 2,800 cycles. After cycling in acidic MCE solution, the films were rinsed with deionized water in order to remove any unbound thiol from the films.

Electrochemical impedance spectroscopy

Impedance measurements were performed using an IVIUM-STAT potentiostat (Ivium Technologies, The Netherlands). The impedance measurements were done in a Faraday cage in a three-electrode cell described in "Electropolymerization of aniline". The impedance spectra were recorded in the frequency range 100 kHz–0.1 Hz (ten frequencies per decade) by using a sinusoidal excitation signal with an ac amplitude of 10 mV.
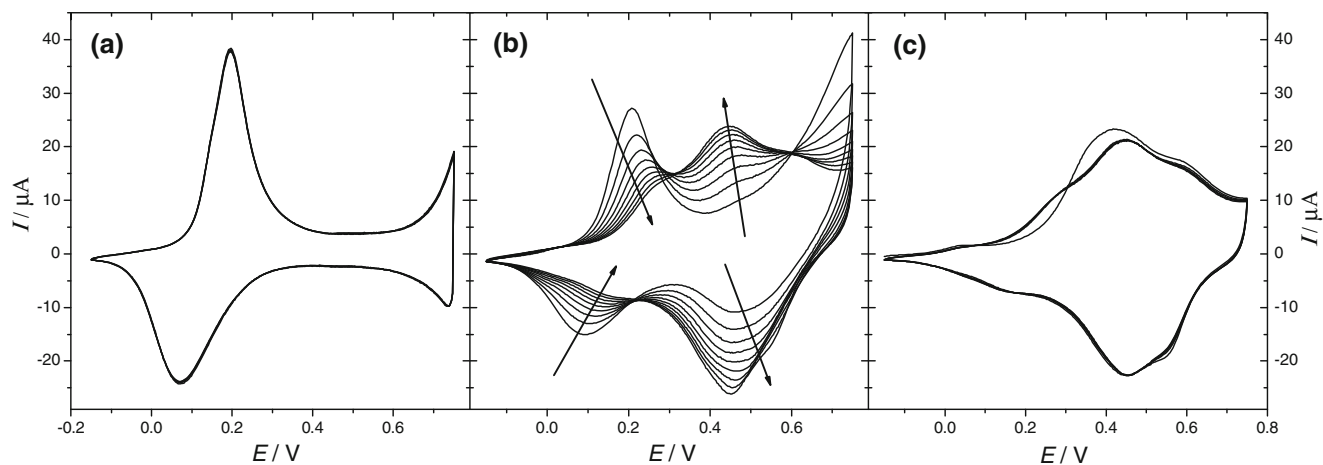
Fig. 1 CV of GC/PANI (50-cycle-PANI film) in **a** 0.5 M H_2SO_4 before thiolation, **b** 10 cycles in 0.1 M MCE+0.5 M H_2SO_4, and **c** 0.5 M H_2SO_4 after thiolation. Scan rate=50 mV/s

The impedance of GC/PANI was measured after different degrees of thiolation were obtained by prior cycling GC/PANI in a mixture of 0.1 M MCE and 0.5 or 1.0 M H_2SO_4 for 10, 50, 100, 200, 300, 700, and 1,600 (1.0 M H_2SO_4) or 2,800 (0.5 M H_2SO_4) cycles. The impedance measurements were done at six different dc potentials (E_{dc}=0.55, 0.45, 0.35, 0.25, 0.15, and −0.15 V) in pure acid solution (without thiol).

Results and discussion

The progress of the thiolation process and subsequent changes in the electrochemical properties of GC/PANI

were followed by CV and EIS. The first studied state of thiolation was achieved after 10 cycles in the acidic MCE mixture, whereafter the thiolated film was washed with water to remove any unbound thiol, followed by CV and impedance spectra which were recorded in fresh 0.5 M and 1.0 M H_2SO_4. The next (higher) state of thiolation was obtained when the film was cycled further for 40 cycles (total of 50 cycles), after which the film was again washed and studied by CV and impedance measurements. These measurements were repeated after a total of 100, 200, 300, and 700 cycles. The last CVs and EISs were measured after a total of 1,600 cycles (1.0 M H_2SO_4) and 2,800 cycles (0.5 M H_2SO_4).

Fig. 2 CVs of **a** GC/PANI (50-cycle-PANI film) in 0.5 M H_2SO_4 and **b** GC/PANI (50-cycle-PANI film) in 1.0 M H_2SO_4 after (*1*) 0, (*2*) 10, (*3*) 50, (*4*) 100, (*5*) 200, (*6*) 300, (*7*) 700, and (*8*) 1,600 (**a**)/2,800 (**b**) cycles in a solution of 0.1 M MCE+0.5 M (**a**)/1.0 M (**b**) H_2SO_4
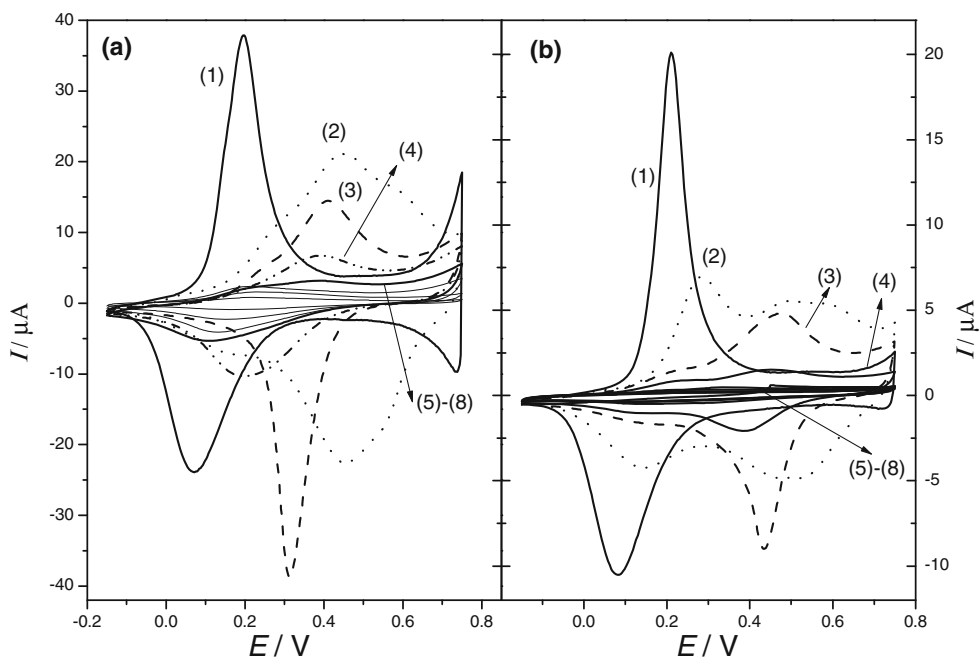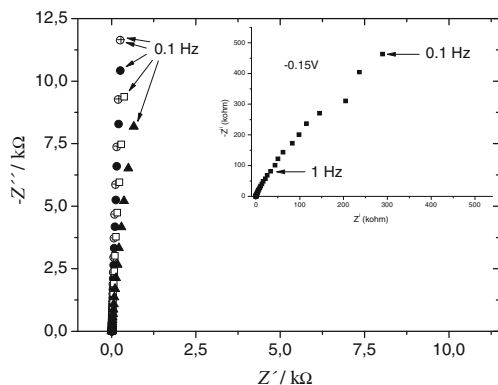
Fig. 3 Electrochemical impedance spectra of intact GC/PANI (50-cycle-PANI film) in 0.5 M H$_2$SO$_4$ at the following dc potentials (E_{dc}): 0.55 V (*filled circle*), 0.45 V (*open circle*), 0.35 V (*plus symbol*), 0.25 V (*open square*), 0.15 (*filled triangle*), and −0.15 V (*filled square*). Frequency range=100 kHz–0.1 Hz

Cyclic voltammetry of GC/PANI

The CV of intact (non-thiolated) GC/PANI in 0.5 M H$_2$SO$_4$ is shown in Fig. 1a. The changes in the voltammogram for the same GC/PANI electrode during CV in acidic MCE solution (10 cycles) are shown in Fig. 1b. Finally, the CV of the thiolated GC/PANI electrode, from Fig. 1b, in MCE-free acid is shown in Fig.1c. The anodic and cathodic peak currents of the main redox peaks of PANI (Fig. 1a) decreased significantly by thiolation with simultaneous appearance of a new redox couple at more positive potential (Fig. 1b). The thiolation process is irreversible (Fig. 1c). During this initial stage of thiolation, which is illustrated in Fig. 1, PANI remains electroactive, but the oxidation (p-doping) of thiolated PANI is shifted to more positive potential compared to intact (non-thiolated) PANI. Thiolation decreases the effective conjugation length of PANI, resulting in a positive shift of the oxidation potential. The initial process of thiolation thus causes a decrease in electroactivity at 0–0.25 V and an increase in electroactivity at 0.25–0.6 V. More extensive thiolation by
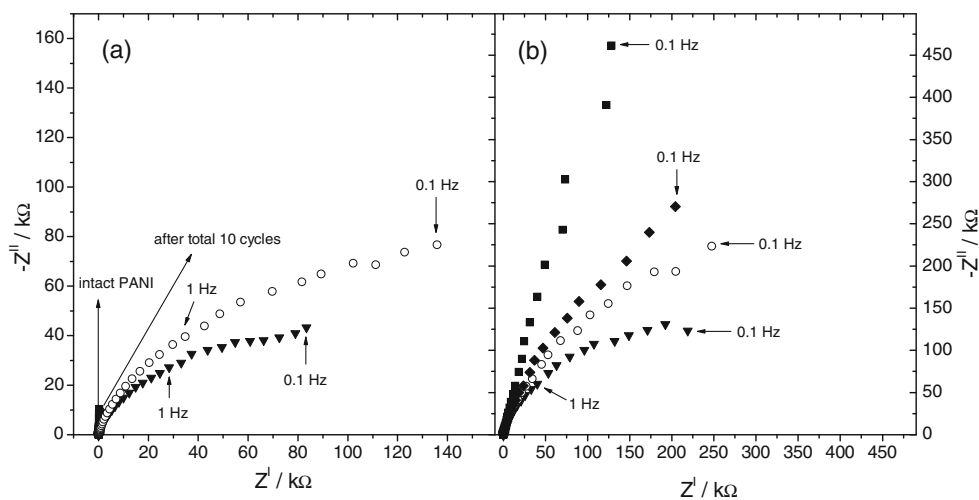
an increasing number of cycles in MCE solution causes a gradual decrease in the electroactivity of PANI in the entire potential range studied (shown in Fig. 2). This indicates that the thiolated monomer units of PANI are not electroactive or that thiolation causes side reactions that lower the electroactivity of thiolated PANI.

The overall effect of thiolation is the reduction of the PANI backbone where quinoid rings are reduced to benzenoid rings while the thiol is bound covalently to the benzene ring [14–18]. We have shown that the same phenomenon of reduction of PANI takes place also with emeraldine salt where no quinoid units are present (Blomquist et al., manuscript submitted for publication). In our earlier work (Blomquist et al., manuscript submitted for publication), we showed that thiolation of PANI can be maximized by potential cycling. Han et al. [14, 15] also maximized thiolation by reoxidation of a partially thiolated PANI either electrochemically (constant potential) or chemically by using *m*-chloroperoxybenzoic acid as the oxidizing compound.

The cyclic voltammograms shown in Fig. 2 indicate further that thiolation initially proceeds fast but gradually slows down. This can be related to the decreasing number of free sites on the PANI backbone available for thiolation and possibly also to a decreased transport rate of MCE in the bulk of the PANI film (and across the PANI/solution interface) due to steric hindrance caused by the MCE substituents bound to PANI.

Impedance spectra of GC/PANI

The impedance spectra of an intact GC/PANI electrode are dominated by capacitive lines close to 90° at all dc potentials measured except at −0.15 V (shown in Fig. 3). This is in good accordance with the earlier impedance measurements for PANI [23–28]. Some impedance spectra of PANI show a high-frequency semicircle [29, 30]. In those cases, however, electropolymerization was done at a higher potential.

Fig. 4 Electrochemical impedance spectra of GC/PANI (50-cycle-PANI film) thiolated gradually by CV in a solution of 0.1 M MCE+0.5 M H$_2$SO$_4$ with **a** 0 (*filled square*), 10 (*filled diamond*), 50 (*filled inverted triangle*), and 100 (*open circle*) cycles and **b** 200 (*filled inverted triangle*), 300 (*open circle*), 700 (*filled diamond*), and 2,800 (*filled square*) cycles. E_{dc}=0.55 V, frequency range=100 kHz–0.1 Hz

Fig. 5 Electrochemical impedance spectra of GC/PANI (50-cycle-PANI film) thiolated gradually by CV in a solution of 0.1 M MCE+1.0 M H_2SO_4 with **a** 0 (*filled square*), 10 (*filled diamond*), 50 (*filled inverted triangle*), and 100 (*open circle*) cycles and **b** 200 (*filled diamond*), 300 (*open square*), 700 (*filled square*), and 1,600 (*filled inverted triangle*) cycles. E_{dc}=0.55 V, frequency range=100 kHz–0.1 Hz
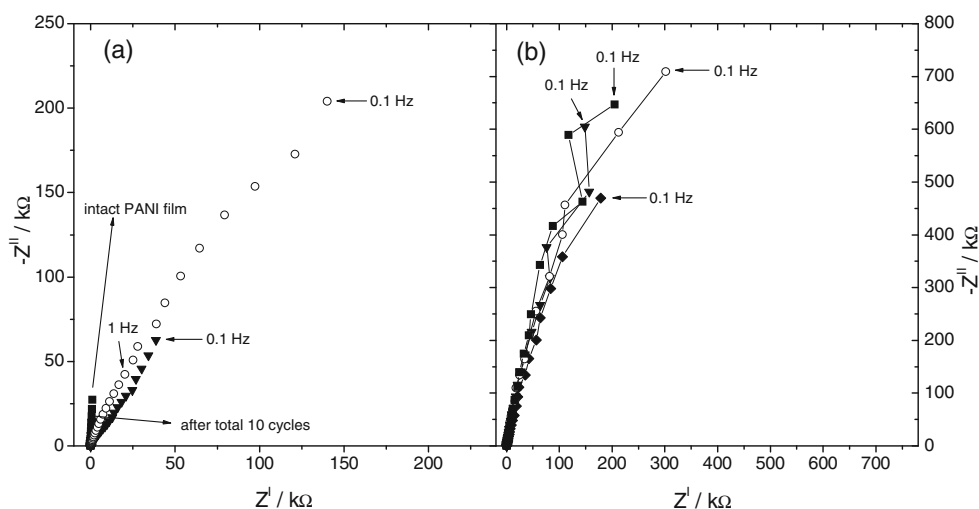
This resulted in the second redox wave for PANI at more positive potentials, which was not observed in the CV of our freshly prepared PANI films (Fig. 1a). The capacitive lines can generally be related to the bulk redox capacitance of PANI because the magnitude of the imaginary impedance was found to decrease with increasing film thickness [27]. The bulk redox capacitance originates from the reversible oxidation (p-doping) of PANI. According to our results, the sulfuric acid concentration did not influence the shape of the impedance spectra of the intact film. This is in good agreement with the results by Rossberg et al. [26]. The impedance spectra at −0.15 V, however, show the beginning of a large (depressed) semicircle with possible contributions from diffusion processes (shown in the inset in Fig. 3). At this dc potential, there is a significant resistance involved, which is due to the fact that PANI is in the non-conducting, leucomeraldine state, i.e., in its fully reduced form at E_{dc}=−0.15 V.

The solution resistance R_s obtained from the intersection with the Z'-axis remains the same in all experiments,

being ~10 and ~6 Ω for 0.5 and 1.0 M H_2SO_4, respectively. Also, the impedance spectra at E_{dc}=−0.15 V where PANI is fully reduced (leucoemeraldine form) remain essentially unchanged for different degrees of thiolation. Therefore, the following discussion is limited to impedance spectra obtained at E_{dc}=0.55, 0.45, 0.35, 0.25, and 0.15 V.

The impedance spectra of GC/PANI at E_{dc}=0.55 V in 0.5 M H_2SO_4 are shown in Fig. 4 and in 1.0 M H_2SO_4 in Fig. 5. As can be seen in those figures, extensive thiolation (> 10 cycles) causes a dramatic increase in the overall impedance of GC/PANI. The corresponding changes in CV were shown in Fig. 2. After extensive thiolation, the impedance spectra of GC/PANI at E_{dc}=0.55 V become similar to those observed for the fully reduced non-thiolated PANI at E_{dc}=−0.15 V (shown in the inset of Fig. 3). The corresponding cyclic voltammograms also show a loss of electroactivity after extensive thiolation (Fig. 2).

As could be seen earlier in Fig. 1, c, the first 10 cycles of thiolation already dramatically changed the shape of the CV
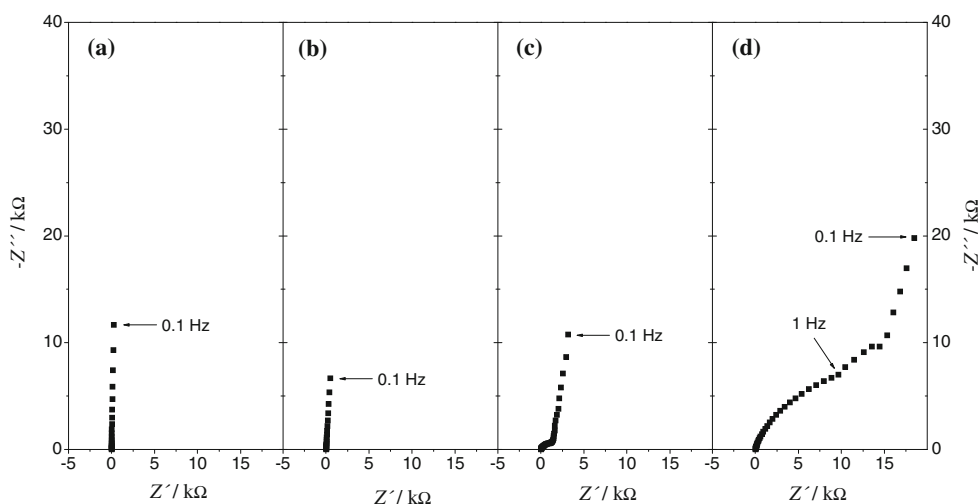

Fig. 6 Electrochemical impedance spectra of GC/PANI (50-cycle-PANI film) after thiolation with **a** 0, **b** 10, **c** 50, and **d** 100 cycles in 0.1 M MCE and 0.5 M H_2SO_4. E_{dc}=0.35 V, frequency range=100 kHz–0.1 Hz
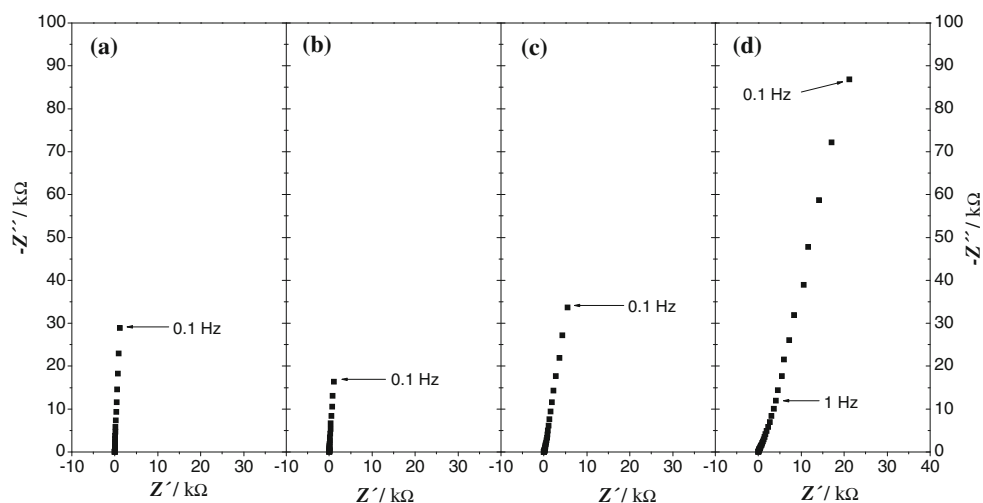
Fig. 7 Electrochemical impedance spectra of GC/PANI (50-cycle-PANI film) after thiolation with **a** 0, **b** 10, **c** 50, and **d** 100 cycles in 0.1 M MCE and 1.0 M H_2SO_4. E_{dc}=0.35 V, frequency range=100 kHz–0.1 Hz

of GC/PANI when the thiolation was done in 0.5 M H_2SO_4. However, as can be seen in Figs. 4 and 5, the impedance spectra of GC/PANI in both 0.5 and 1.0 M H_2SO_4 still show mainly capacitive lines and only a slight increase in the resistance after 10 cycles of thiolation. It was found that at E_{dc}=0.55, 0.45, and 0.35 V, the imaginary part of the impedance, $-Z''$, decreased at low frequencies after thiolation (10 cycles), indicating that the capacitance of the PANI film increased at these potentials. This is in good agreement with the appearance of the new redox couple in CV at 0.3–0.6 V (Fig. 1). At E_{dc}=0.25 V, the value of $-Z''$ increased slightly and the increase was more significant at E_{dc}=0.15 V, which also correlates well with the decrease in the CV peaks at 0–0.3 V corresponding to the leucoemeraldine–emeraldine redox pair of PANI (Fig. 1). The overall changes in the impedance spectra are thus in good agreement with the changes in CV during the initial stages of thiolation (10 cycles) (Blomquist et al., manuscript submitted for publication).

The influence of the acid concentration (0.5 and 1.0 M H_2SO_4) on the impedance spectra of GC/PANI and for differ-ent degrees of thiolation (0, 10, 50, and 100 cycles) is illus-trated in Figs. 6 and 7 at E_{dc}=0.35 V and in Figs. 4a and 5a at E_{dc}=0.55 V. The initial increase in the bulk redox capacitance of PANI (at E_{dc}=0.35 V) after 10 cycles of thiolation can be clearly seen in Figs. 6 and 7. At E_{dc}=0.35 V, after 50 cycles of thiolation, the impedance spectrum for GC/PANI in 0.5 M H_2SO_4 shows a charge transfer semicircle (Fig. 6) which is not visible for GC/PANI in 1.0 M H_2SO_4 (Fig. 7). Furthermore, the capacitance of PANI is higher in 0.5 M H_2SO_4 (Fig. 6) than in 1.0 M H_2SO_4 (Fig. 7) during the thiolation process (0–100 cycles). This indicates that thiolation proceeds faster in the more concentrated acid, which is also seen in the cyclic voltammograms (Fig. 2). Also, the impedance spectra at E_{dc}= 0.55 V shown in Figs. 4 and 5 indicate that thiolation proceeds faster in 1.0 M H_2SO_4 than in 0.5 M H_2SO_4. According to the impedance spectra in Fig. 5, the PANI film was totally reduced and the electroactivity was lost after thiolation for 1,500 cycles in 1.0 M H_2SO_4+0.1 M MCE. In the case of 0.5 M H_2SO_4+ 0.1 M MCE, 2,800 cycles were needed for the total reduction of the PANI film (Fig. 4).

Fig. 8 Electrochemical impedance spectra of GC/PANI (50-cycle-PANI film) after thiolation with 100 cycles in 0.1 M MCE and 0.5 M H_2SO_4. **a** E_{dc}=0.55 V (*filled square*), **b** E_{dc}=0.45 V (*filled circle*), 0.35 V (*open square*), 0.25 V (*filled triangle*), and 0.15 V (*open circle*). Frequency range=100 kHz–0.1 Hz
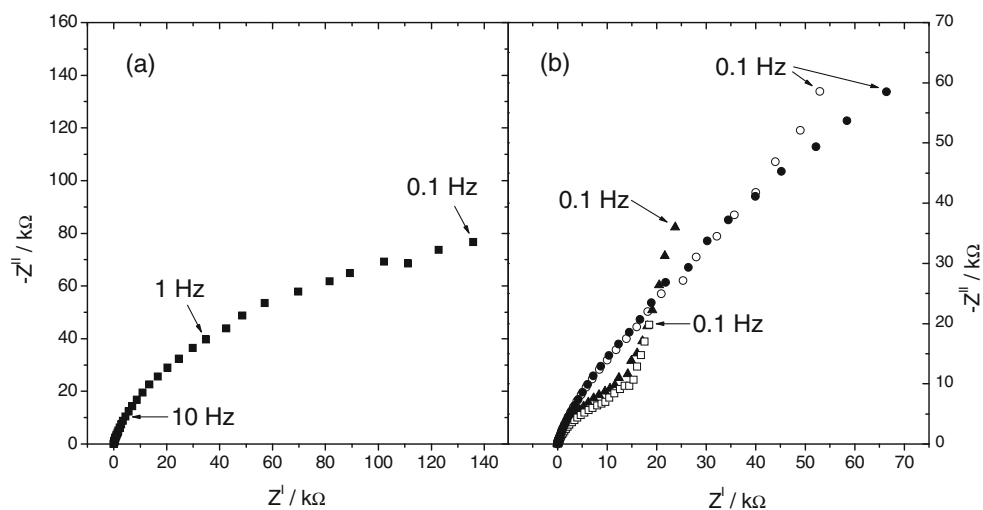
The impedance spectra of GC/PANI at an intermediate degree of thiolation (100 cycles) in 0.5 M H_2SO_4 at different dc potentials are shown in Fig. 8. At E_{dc}=0.35 and 0.25 V, there is a charge transfer semicircle followed by a capacitive line. A larger semicircle is observed at E_{dc}=0.55 V. At E_{dc}=0.15 and 0.45 V, the semicircle is overlapping with a 45° diffusion line. At this degree of thiolation (100 cycles), PANI thus shows the highest capacitance around E_{dc}=0.25–0.35 V, while at higher and lower potentials the charge transfer and transport are more restricted. This is in good agreement with the voltammetric results presented in Fig. 2a.

Conclusions

When the PANI film was thiolated by CV with an increasing number of cycles in acidic MCE solution, there was an initial increase in the electroactivity of PANI at 0.25–0.6 V up to a certain number of cycles. Upon further thiolation, the electro-activity of PANI decreased in the entire potential range studied (−0.15–0.75 V), which was related to a decrease in the bulk redox capacitance and increase in the resistance of PANI as shown by EIS. After extensive thiolation, the impedance spectra become similar to those of the fully reduced (non-conducting) leucoemeraldine state of PANI. Thiolation of PANI was found to be significantly faster in 1.0 M H_2SO_4 compared to 0.5 M H_2SO_4 as supporting electrolyte. Extensive functionalization of PANI films via thiolation thus seems to be most suitable for such applications where a low electro-activity of PANI is acceptable or even preferred.

References

1. Orazem ME, Tribollet B (2008) Electrochemical impedance spectroscopy. Wiley, Hoboken
2. Inzelt G, Láng GG (2010) Electrochemical impedance spectroscopy (EIS) for polymer characterization. In: Cosnier S, Karyakin A (eds) Electropolymerization. Wiley, Weinheim, pp 51–76
3. Lindfors T, Ivaska A (2002) J Electroanal Chem 531:43–52
4. Miras MC, Acevedo DF, Monge N, Frontera E, Rivarola CR, Barbero CA (2008) The Open Macromol J 1:58–73
5. Blomquist M, Lindfors T, Ivaska A (2007) Synth Met 157:974–983
6. Blomquist M, Lindfors T, Vähäsalo L, Pivrikas A, Ivaska A (2006) Synth Met 156:549–557
7. Blomquist M, Lindfors T, Latonen R-M, Bobacka J (2009) Synth Met 159:96–102
8. Barbero C, Salavagione HJ, Acevedo DF, Grumelli DE, Garay F, Planes GA, Morales GM, Miras MC (2004) Electrochim Acta 49:3671–3686
9. Pividori M, Merkoçi A, Alegret S (2000) Biosens Bioelectron 15:291–303
10. Herne TM, Tarlov MJ (1997) J Am Chem Soc 119:8916–8920
11. Peeters S, Stakenborg T, Reekmans G, Laureyn W, Lagae L, Van Aerschot A, Van Ranst M (2008) Biosens Bioelectr 24:72–77
12. Bobacka J (2006) Conjugated polymer chemical sensors. In: Grimes CA, Dickey EC, Pishko MV (eds) Encyclopedia of sensors, vol 2. American Scientific, San Diego CA, pp 279–294
13. Zhou Y, Yu B, Guiseppi-Elie A, Sergeyev V, Levon K (2009) Biosens Bioelectr 24:3275–3280
14. Han C-C, Jeng R-C (1997) Chem Commun (6)553–554
15. Han C-C, Hseih W-D, Yeh J-Y, Hong S-P (1999) Chem Mater 11:480–486
16. Han C-C, Hong S-P, Yang K-F, Bai M-Y, Lu C-H, Hung C-S (2001) Macromolecules 34:587–591
17. Bergman B, Hanks TW (2000) Macromolecules 33:8035–8042
18. Su Z, Huang J, Xie Q, Fang Z, Zhou C, Zhou Q, Yao S (2009) Phys Chem Chem Phys 11:9050–9061
19. Garnier F, Korri-Youssufi H, Srivastava P, Mandrand B, Delair T (2009) Synth Met 100:89–94
20. Lubert K-H, Dunsch L (1998) Electrochim Acta 43:813–822
21. Grzeszczuk M, Szostak R (2004) J Electroanal Chem 571:51–57
22. Lindfors T, Harju L (2008) Synth Met 158:233–241
23. Fiordiponti P, Pistoia G (1989) Electrochim Acta 34(2):215–221
24. Inzelt G, Láng G, Kertész V, Bácskai J (1993) Electrochim Acta 38:2503–2510
25. Grzeszczuk M, Żabińska-Olszak G (1993) J Electroanal Chem 359:161–174
26. Roßberg K, Paasch G, Dunsch L, Ludwig S (1998) J Electroanal Chem 443:49–62
27. Dinh HN, Vanýsek P, Birss VI (1999) J Electrochem Soc 146 (9):3324–3334
28. Dinh HN, Birss VI (2000) J Electrochem Soc 147(10):3775–3784
29. Hao Q, Lei W, Xia X, Yan Z, Yang X, Lu L, Wan X (2010) Electrochim Acta 55:632–640
30. Zou W, Wang W, He B, Sun M, Wang M, Liu L, Xu X (2010) J Electroanal Chem 641:111–118